Int. J. Electrochem. Sci., 7 **(2012)** 686 - 696

International Journal of
ELECTROCHEMICAL
SCIENCE
www.electrochemsci.org

Formation of Disperse Silver Deposits by the Electrodeposition Processes at High Overpotentials

Konstantin I. Popov[1,2,*] *, Predrag M. Živković*[2] *and Nebojša D. Nikolić*[1]

[1] ICTM- Institute of Electrochemistry, University of Belgrade, Njegoševa 12, 11000 Belgrade, Serbia
[2] Faculty of Technology and Metallurgy, University of Belgrade, Karnegijeva 4, 11120 Belgrade, Serbia
[*]E-mail: kosta@tmf.bg.ac.rs

Received: 11 November 2011 / *Accepted:* 21 December 2011 / *Published:* 1 January 2012

In this study, electrodeposition of silver from nitrate solution at the high overpotentials was analyzed. Morphologies of silver deposits obtained at the different overpotentials and with the different electrodeposition times were examined using the technique of scanning electron microscopy (SEM). The different disperse morphological forms, such as granules, needle-like and spongy-dendritic ones were formed during silver electrodeposition from this solution. The size of granules decreased and their number increased with the increase of overpotential of electrodeposition. With the increasing overpotential, the induction time for the appearance of spongy-dendritic forms decreased with a tendency to increase their ramification. Mathematic model describing the mechanism of metal electrodeposition at the high overpotentials is proposed and discussed on the basis of the obtained silver surface morphology.

Keywords: Silver; electrodeposition; granules; spongy-dendritic form; scanning electron microscopy.

1. INTRODUCTION

There are two conditions under which the particles of active metal placed on the surface of the inert macroelectrode can represent microelectrodes. The first condition is that a substrate is conductive but inert relative to the process under consideration. The second one is fulfilled when the grains are small and far enough from each other. Electrodeposition on the macroelectrode of metal which deposition process is characterized by the very large exchange current density value can be under complete diffusion control at all deposition overpotentials. Simultaneously, electrodeposition to the microelectrode can be under complete activation control if the radius of the microelectrode is sufficiently low. In the conditions of the low nucleation rate on the inert substrate, electrodeposition to the formed nuclei is under complete activation control up to some critical value of grain radius. At the

larger grain radii electrodeposition enters the mixed activation-diffusion control. Then, the independent spherical diffusion layer is formed inside a diffusion layer of the macroelectrode around each of them, as in the case of growing dendrites [1 – 3] or during induction time in the process of spongy deposits formation [4 – 6]. Inside such spherical diffusion layer all process as in the diffusion layer of the macroelectrode can occur. The moment when the nondendritic surface roughness amplification starts on the microelectrode marks the initiation of the spongy deposits growth on the macroelectrode at low overpotentials [7]. It was shown [4, 5] that the mechanism of dendritic-spongy deposit formation at low overpotentials can be succesfully illustrated by the physical model and that calculations derived for the real system can be applied for the model.

Electrodeposition of silver from nitrate solutions belongs to the fast electrochemical processes because it is characterized by the large exchange current density, j_0 [8]. The processes of silver electrodeposition from these solutions are widely studied using both the constant [9 – 13] and periodically changing regimes of electrolysis [14, 15], and many of disperse morphological forms, such as granules, spongy, dendrites, were formed by these regimes of electrolysis. In the constant regimes of electrolysis, all investigations of the processes of silver electrodeposition were performed at low overpotentials. Meanwhile, the processes of silver electrodeposition at the high overpotentials are completely unexplored. For that reason, the aim of this study is to consider mechanism of the formation of silver dendritic-spongy deposits at high overpotentials.

2. EXPERIMENTAL PART

Silver was electrodeposited from solution containing 0.50 M $AgNO_3$ in 0.20 M HNO_3 on the stationary graphite working electrodes (length 25 mm, diameter 0.70 mm). Electrodeposition of silver was carried out potentiostatically using WENKING 7103 GIRH potentiostat and PAR 175 universal programmer. The counter electrode was a foil of pure silver of 0.80 dm^2 surface area placed close to the walls of the cell, while the reference electrode was a silver wire which the tip was positioned at a distance of 0.2 cm from the surface of the working electrode. The working electrode was situated in the centre of cell at the same location for each experiment.

Doubly distilled water and analytical grade chemicals were used for the preparation of the solution for electrodeposition of silver. All experiments were performed in an open cell at the room temperature.

The deposits of silver were investigated by means of the scanning electron microscope (SEM) using JEOL JSM-6610 LV microscope.

3. RESULTS AND DISCUSSION

Figure 1 shows the silver deposit obtained at an overpotential of 100 mV with electrodeposition time of 180 s. From Fig. 1, it can be clearly seen that silver granules were formed during electrodeposition at this overpotential.

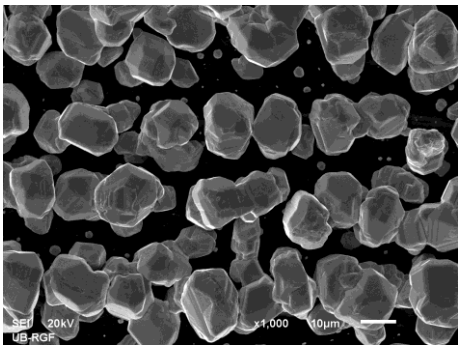

Figure 1. Silver deposit obtained at an overpotential of 100 mV with electrolysis time of 180 s.

Morphologies of silver deposits obtained at an overpotential of 200 mV with electrodeposition times of 1 and 10 s are shown in Fig. 2a and b, respectively. The strong effect of the electrodeposition time on morphology of electrodeposited silver is clearly seen from Fig. 2. The silver granules similar to those formed at 100 mV were obtained with electrolysis time of 1 s (Fig. 2a). On the other hand, the needle-like dendrites were primarily formed with the electrodeposition time of 10 s (Fig. 2b).

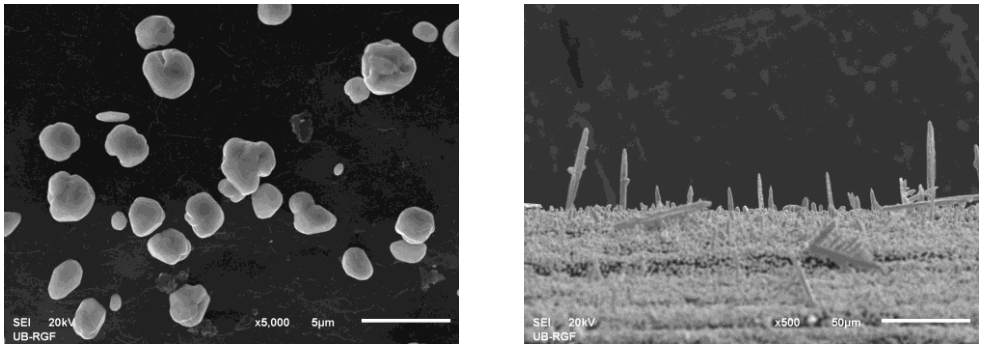

A B

Figure 2. Silver deposits obtained at an overpotential of 200 mV. Deposition time: a) 1 s, and b) 10 s.

Figure 3 shows silver deposits obtained at an overpotential of 300 mV with electrodeposition times of 1 s (Fig. 3a), 3 s (Fig. 3b) and 5 s (Fig. 3c). As expected, individual silver granules were formed with the electrolysis time of 1 s (Fig. 3a). The prolongation of the electrodeposition time led to the formation of spongy-dendritic forms as shown in Fig. 3b. The branching of these forms increased with the further prolongation of electrodeposition time (Fig. 3c). Anyway, the conditions of the spherical diffusion control around the growing grains are fulfilled during electrodeposition at an overpotential of 300 mV causing the formation of dendritic-spongy deposits what is confirmed by the growth of these forms in all direction.

The similar silver surface morphologies were developed during silver electrodeposition at an overpotential of 700 mV, as shown in Fig. 4.

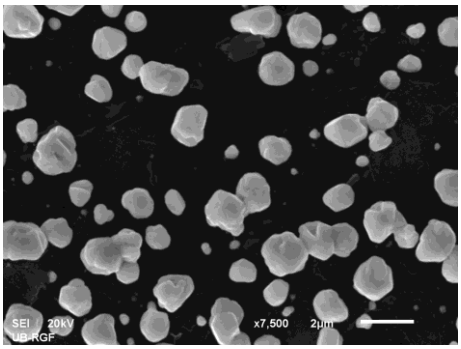

A

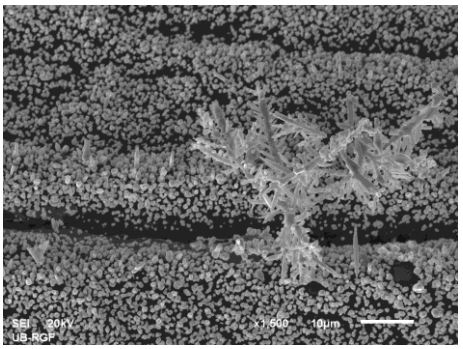

B

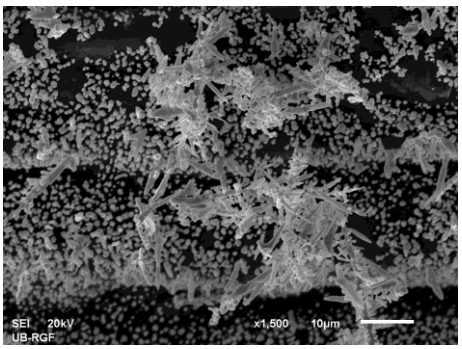

C

Figure 3. Silver deposits obtained at an overpotential of 300 mV. Deposition time: a) 1 s, b) 3 s, and c) 5 s.

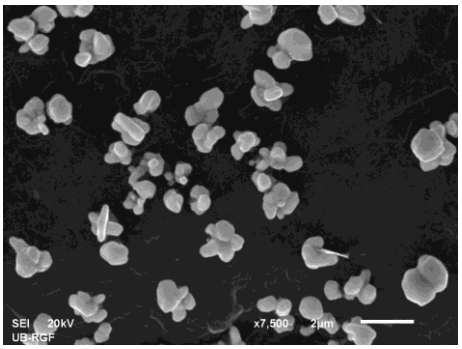

A

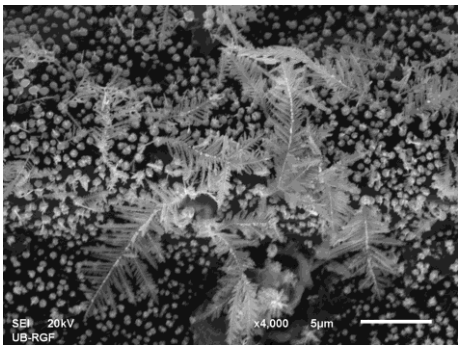

B

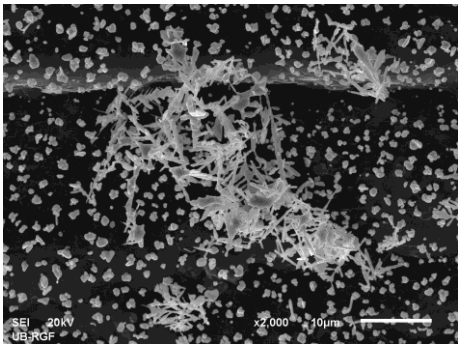

C

Figure 4. Silver deposits obtained at an overpotential of 700 mV. Deposition time: a) 0.15 s, b) 0.30 s, and c) 0.50 s.

The number of the formed silver granules increased while their size decreased with the increase of overpotential of electrodeposition, what is understandable due to the dependence of the nucleation rate on overpotential of electrodeposition [9]. With the increasing overpotential, the induction time for the beginning of the spongy-dendritic growth decreased, while their branching was increased. In order to explain the formed morphologies of silver deposits, the following mathematical model considering silver electrodeposition at the high overpotentials was proposed.

According to Barton and Bockris [1], if an electrochemical process on the microelectrode with

$$r_m \leq 55\ \mu m \tag{1}$$

is under complete diffusion control, then a spherical diffusion layer of the thickness equal to the radius of microelectrode, r_m, is formed around the microelectrode [1]. The condition (1) is always satisfied because

$$r_m << \delta \tag{2}$$

where δ is the thickness of diffusion layer of the macroelectrode. Hence, it can be expected that the diffusion layers of spherical particles will not overlap if

$$a > 4r_m \tag{3}$$

where a is the distance between the centers of the closest particles.

Then, the common diffusion layer of the macroelectrode will be formed at the longer electrodeposition times, as schematically presented in Fig. 5. The silver deposits shown in Figs. 3 and 4 represent a fine experimental verification of this case. The growth of dendrites in all directions means the existence of the spherical diffusion control around the growing grains in the initial stage of the electrodeposition.

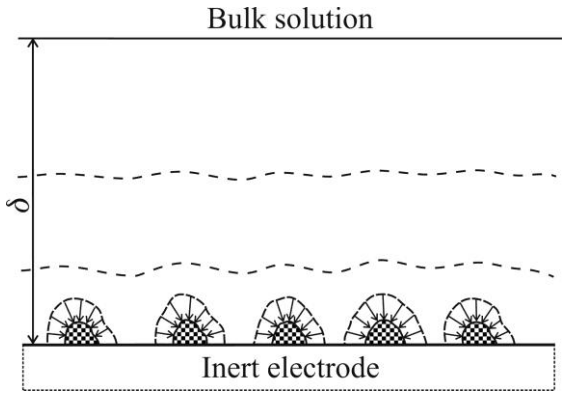

Figure 5. Schematic presentation of formation of diffusion layer of the inert macroelectrode covered with active grains at $a > 4r_m$.

On the other hand, if $a < 4r_m$ the diffusion layers of the microelectrodes are not formed and the diffusion layer of the macroelectrode is formed as on the massive electrode of active metal. This case is schematically presented in Fig. 6. The experimental verification of this case can be found in the shape of needle-like dendrites shown in Fig. 2b. The shape of these dendrites clearly indicates that the spherical diffusion layer is not formed around the growing grains before the formation of the diffusion layer of the macroelectrode. Anyway, the process of electrodeposition inside the diffusion layer of the macroelectrode was confirmed by the growth of the needle-like dendrites towards the bulk of solution.

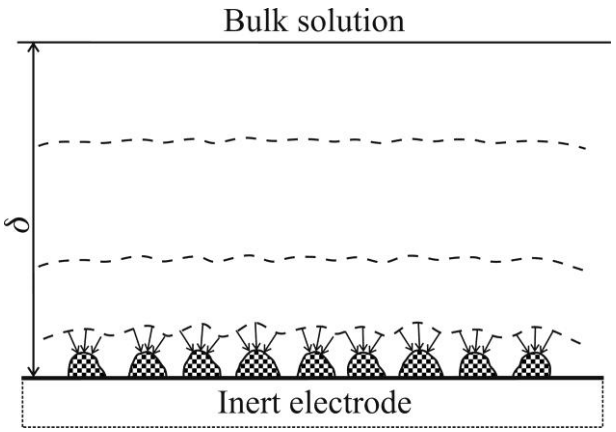

Figure 6. Schematic presentation of formation of diffusion layer of the inert macroelectrode covered with active grains at $a < 4r_m$

If a cathodic current density and overpotential are taken as positive, the current density to the macroelectrode of the massive metal, j, is given by [5]:

$$j = \frac{j_0 f_c}{1 + \frac{j_0 f_c}{j_L}} \tag{4}$$

where j_0 and j_L are the exchange current density and the limiting diffusion current density for the process under consideration, respectively, and

$$f_c >> f_a \tag{5}$$

where

$$f_c = 10^{\frac{\eta}{b_c}} \tag{6}$$

and

$$f_a = 10^{-\frac{\eta}{b_a}} \tag{7}$$

In Eqs. (6) and (7) η is the overpotential while b_c and b_a are the cathodic and anodic Tafel slopes, respectively.

The limiting diffusion current density, j_L, to the macroelectrode is given by:

$$j_L = \frac{nFDC_0}{\delta} \tag{8}$$

while the limiting diffusion current density to the spherical microelectrode, $j_{L,m}$, in bulk solution is:

$$j_{L,m} = \frac{nFDC_0}{r_m} \tag{9}$$

where n is the number of transferred electrons, F is the Faraday constant and D and C_0 are the diffusion coefficient and the bulk concentration of depositing ions, respectively.

Then, from Eqs. (8) and (9), the limiting diffusion current density to the microelectrode, $j_{L,m}$, can be related to j_L as:

$$j_{L,m} = \frac{\delta}{r_m} j_L \tag{10}$$

For a microelectrode, Eq. (4) can be rewritten in the form:

$$j_m = \frac{j_0 f_c}{1 + \frac{j_0 f_c}{j_L} \cdot \frac{r_m}{\delta}} \tag{11}$$

where j_m is the current density to the microelectrode. It is obvious from Eqs. (4) and (11) that electrodeposition process on the macroelectrode can be under complete diffusion control if:

$$\frac{j_0 f_c}{j_L} >> 1 \tag{12}$$

Simultaneously, at the same overpotential, electrochemical process on the microelectrode can be under pure activation control if the conditions:

$$\frac{j_0 f_c}{j_L} \cdot \frac{r_m}{\delta} << 1 \tag{13}$$

or

$$\frac{r_m}{\delta} \to 0 \tag{14}$$

are satisfied.

The conditions given by Eqs. (13) and (14) are fulfilled by the formation of the metal nuclei during the initial stage of electrodeposition on the inert substrate [5]. These nuclei will behave as microelectrodes due to their complete independent growth before the formation of the diffusion layer of the macroelectrode.

The radius r_0 of the initial stable nucleus, at overpotential η is given by Eq. (15) [16]:

$$r_0 = \frac{2\sigma V}{nF} \tag{15}$$

where σ is the surface energy and V is the molar volume of the metal. The radius of the growing nucleus will vary with the time according to Eq. (16) [17]:

$$r_m = r_0 + \frac{V}{nF} j_0 f_c t \tag{16}$$

or

$$r_m \approx \frac{V}{nF} j_0 f_c t \tag{17}$$

because r_0 is extremely low.

Equations (11), (13), (16) and (17) are only approximation at the lower electrodeposition times because the effect of surface energy has not been considered. At higher electrodeposition times the surface energy term can be neglected [1], and then, these equations are valid.

An increase in r_m leads to a decrease of $j_{L,m}$ and at sufficiently large r_m electrochemical deposition process is under mixed activation-diffusion control. It can be assumed that this will happen when

$$j_m > \kappa j_{L,m} \tag{18}$$

where $0 < \kappa < 1$. By combining Eqs. (11) and (18) one obtain

$$r_{c,m} \approx \frac{j_L \kappa \delta}{j_0 f_c (1-\kappa)} \tag{19}$$

where $r_{c,m}$ is the radius of the growing nucleus when the process is under mixed or spherical diffusion control. According to Barton and Bockris [1], the diffusion layer around such grain forms

very fast. The further combination of Eqs. (17) and (19) gives the corresponding induction time, t_i, given by:

$$t_i = \frac{j_L}{j_0^2} \frac{\kappa F \delta}{V f_c^2 (1-\kappa)} \tag{20}$$

For sufficiently high overpotentials, Eqs. (19) and (20) can be rewritten in the forms [6]:

$$r_{c,m} = \frac{j_L}{j_0} \frac{\delta}{4 f_c} \tag{21}$$

and

$$t_i = \frac{j_L}{j_0^2} \frac{nF\delta}{4V f_c^2} \tag{22}$$

for $\kappa = 0.2$.

At $r < r_{c,m}$ and $t < t_i$ the deposition on the growing grain is under activation control.

Hence, if $a > 4r_m$ and $r_m > r_{c,m}$, the spherical diffusion layer around microelectrode can be formed.

The nucleus of spongy-dendritic deposit, *i.e.* hedgehog-like particle, appears when amplification of surface coarseness on the nucleus growing in the spherical diffusion control starts to grow. It was already shown [6] that the growth of amplification is very fast so the induction time when growing nucleus enters the mixed control can be taken as induction time of spongy-dendritic formation. It follows from Eqs. (17) and (18) that $r_{c,m}$ and t_i decrease with the increasing overpotential.

On the other hand, it was also shown [5] that a spongy-dendritic deposit can be only formed if around each grain with radius r_c, growing under spherical diffusion control, a diffusion layer of the same thickness is formed. This condition is fulfilled if

$$N \le \frac{1}{(4r_{c,m})^2} \tag{23}$$

where N is the number of grain per square centimeter of the macroelectode. It is obvious that condition (23) is the same as $a \ge 4r_m$. Hence, electrodeposition in the spherical diffusion control on the growing grain is possible if conditions both (19) and (23) are satisfied. Simultaneously, the nucleation law can be written in the form [18]:

$$N = N_0\left[1 - e^{-At}\right] \tag{24}$$

where

$$A = K_1 j_0 e^{-\frac{K_2}{\eta^2}} \tag{25}$$

and N_0 is the maximal number of active sites for the selected value of overpotential, while K_1 and K_2 are constants.

Spongy-dendritic deposits formation is possible if

$$N_0\left[1-e^{-At_i}\right] < \frac{1}{4r_{c,m}^2} \tag{26}$$

and

$$At_i \approx 0 \tag{27}$$

This happens at sufficiently high overpotentials where $K_2/\eta^2 \rightarrow 0$, $A \rightarrow K_1 j_0$ and $t_i \rightarrow 0$. Hence, the spongy deposit formation at high overpotentials starts at very low deposition times, when the spherical diffusion layer formed around grains do not overlap. The critical overpotential of the spongy-dendritic formation can be obtained by substitution of $r_{c,m}$ from Eq. (19) and t_i from Eq. (20) in Eq. (27) and by the further calculation. If this overpotential is larger than critical one for instantaneous dendritic growth, the dendrite-spongy nuclei can be formed over inert substrate.

Finally, the fact that $r_{c,m}$ and t_i (Eqs. (20) and (21)) decrease with the increasing overpotential can be verified by Figs. 3 and 4.

4. CONCLUSION

Morphologies of electrodeposited silver from solution containing 0.50 M $AgNO_3$ in 0.20 M HNO_3 at overpotentials of 100, 200, 300 and 700 mV were analyzed using the scanning electron microscopy (SEM) technique. The different disperse morphologies of silver deposits, such as granules, needle-like and spongy-dendritic morphological forms were formed by silver electrodeposition under these electrodeposition conditions. On the basis of the obtained silver surface morphologies, mathematic model considering metal electrodeposition characterized by the large exchange current density on the inert substrates at the high overpotentials was proposed.

ACKNOWLEDGEMENT
The work was supported by the Ministry of Education and Science of the Republic of Serbia under the research project: "Electrochemical synthesis and characterization of nanostructured functional materials for application in new technologies" (No. 172046).

References

1. J.L. Barton and J. O'M. Bockris, *Proc. Roy. Soc.*, A268 (1962) 485.

2. J.W. Diggle, A. R. Despić and J. O'M Bockris, *J. Electrochem. Soc.*, 116 (1969) 1503.
3. K.I. Popov, V. Radmilović, B.N. Grgur and M.G. Pavlović, *J. Serb. Chem. Soc.*, 59 (1994) 47.
4. K.I. Popov, N.V. Krstajić and M.I. Čekerevac, *J. Appl. Electrochem.*, 14 (1986) 771.
5. K.I. Popov and N.V. Krstajić, *J. Appl. Electrochem.*, 13 (1983) 775.
6. K.I. Popov, N.V. Krstajić and S.R. Popov, *J. Appl. Electrochem.*, 15 (1985) 151.
7. K.I.Popov, S.S.Djokić and B.N.Grgur, *Fundamental Aspects of Electrometallurgy*, Kluwer Academic/Plenum Publishers, New York (2002).
8. K.I. Popov, N.V. Krstajić and S.R. Popov, *Surf. Technol.*, 20 (1983) 203.
9. K.I. Popov, B.N. Grgur, E.R. Stojilković, M.G. Pavlović and N.D. Nikolić, *J. Serb. Chem. Soc.*, 62 (1997) 433.
10. A.T. Dimitrov, S. Hadži-Jordanov, K.I. Popov, M.G. Pavlović and V. Radmilović, *J. Appl. Electrochem.*, 28 (1998) 791.
11. K.I. Popov, M.G. Pavlović, B.N. Grgur, A.T. Dimitrov and S. Hadži-Jordanov, *J. Appl. Electrochem.*, 28 (1998) 797.
12. V. Radmilović, K.I. Popov, M.G. Pavlović, A. Dimitrov and S. Hadži-Jordanov, *J. Solid State Electrochem.*, 2 (1998) 162.
13. S.S. Djokić, N.D. Nikolić, P.M. Živković, K.I. Popov and N.S. Djokić, *ECS Transactions*, 33 (2011) 7.
14. K.I. Popov, M.G. Pavlović, E.R. Stojilković and V. Radmilović, *J. Serb. Chem. Soc.*, 61 (1996) 47.
15. A.T. Dimitrov, P. Paunović, O. Popovski, D. Slavkov, Ž. Kamberović and S. Hadži Jordanov, *J. Serb. Chem. Soc.*, 74 (2009) 279.
16. S. Toshev and I. Markov, *Electrochim. Acta*, 12 (1967) 489.
17. J.O`M. Bockris, Z. Nagy and D. Dražić, *J. Electrrochem. Soc.*, 120 (1973) 30.
18. M. Fleischman ad H.R. Thirsk, *Electrochim. Acta*, 1 (1959) 146.